Materials Science

DOI: 10.1002/ange.200601617

Metal-Compound-Induced Vesicles as Efficient Directors for Rapid Synthesis of Hollow Alloy Spheres**

*Xuanjun Zhang and Dan Li**

Vesicles in aqueous solutions are fascinating supramolecular self-assembled structures that have extraordinary potential for applications such as microreactors and nanodevices for encapsulation and controlled release.[1–5] Vesicles can form in dilute solution from different surfactants or phospholipids owing to their amphiphilic character.[6] Some ligands with long alkyl chains can form vesicles upon coordination with metal ions.[7] Vesicles can also form from nanoclusters by self-assembly.[8] Quaternary ammonium ions with short alkyl chains do not form vesicles in the absence of other surfactants. We found that tetrabutylammonium bromide (Bu_4NBr) can assembly rapidly into vesicles in water when mixed with some metal compounds such as $PdCl_2$, $K[AuCl_4]$, $AgNO_3$, $K_2[PtCl_4]$, or the mixtures of these compounds. These metal-compound-induced vesicles can be applied as efficient directors for the rapid synthesis of hollow alloy spheres.

The vesicle formation after the addition of metal compounds into a Bu_4NBr solution was evidenced by turbidity of the solutions and the distinct red shifts of the UV/Vis absorption (Figure 1). The absorbance of the $K[AuCl_4]$ solution peaked at around 223 and 304 nm. When mixed with KBr solution, the absorbance peaks shifted to 257 and 381 nm, respectively, which is ascribed to the replacement of the Cl^- ligand by Br^-, which has a weaker ligand field and leads to a smaller splitting of the Au^{III} d orbitals. Broad absorption peaks with large red shifts were observed after the addition of Bu_4NBr solution. This phenomenon was also observed for the addition of Bu_4NBr to $PdCl_2$, $AgNO_3$, or the mixtures of these salts, and also led to turbidity of the solutions. The formation of vesicles was visualized by transmission electron microscopy (TEM) and scanning electron microscopy (SEM) measurements. The sizes of the vesicles were found to depend on their composition. Representative TEM images of vesicles induced by $PdCl_2/K[AuCl_4]/AgNO_3$, and $PdCl_2/K[AuCl_4]/AgNO_3/K_2[PtCl_6]$ (Figure 2a and b, respectively) reveal hollow vesicles with sizes of approximately 100 nm and 400–500 nm, respectively. SEM images show that vesicles induced by $PdCl_2/K[AuCl_4]/AgNO_3$ are relatively uniform spheres with sizes agreeing with those observed in the TEM measurements (Figure 2c). In contrast, the vesicles formed in a $K_2[PtCl_4]/Bu_4NBr$ system exhibited a large size distribution (20 nm to 2 μm), and the formation process is relatively slow (more than 20 minutes). Some representative large vesicles (> 1 μm) are shown in Figure 2d;

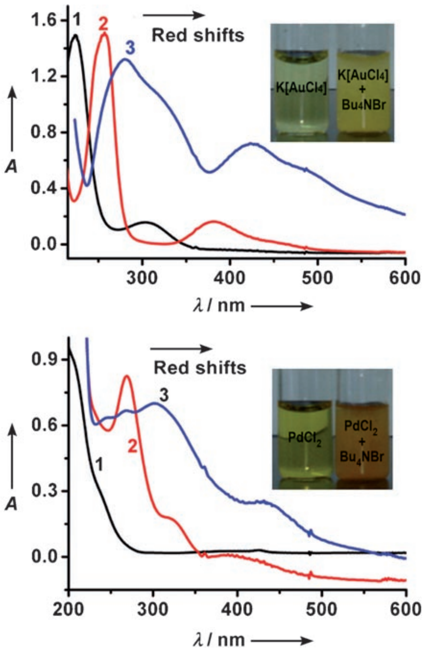

Figure 1. Top: UV/Vis spectra of solutions of $K[AuCl_4]$ (1), $K[AuCl_4]+KBr$ (2), and $K[AuCl_4]+KBr+Bu_4NBr$ (3); Inset: photograph of $K[AuCl_4]$ and $K[AuCl_4]+Bu_4NBr$ solutions. Bottom: UV/Vis spectra of solutions of $PdCl_2$ (1), $PdCl_2+KBr$ (2), and $PdCl_2+KBr+Bu_4NBr$ (3); Inset: photograph of $PdCl_2$ and $PdCl_2+Bu_4NBr$ solutions.

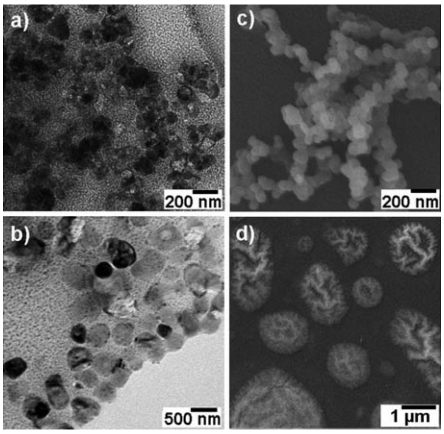

Figure 2. TEM images of vesicles induced by the mixture of $PdCl_2/K[AuCl_4]/AgNO_3$ (a) and $PdCl_2/K[AuCl_4]/K_2[PtCl_6]/AgNO_3$ (b); SEM images of the vesicles induced by $PdCl_2/K[AuCl_4]/AgNO_3$ (c) and $K_2[PtCl_4]$ (d).

---

[*] Dr. X. Zhang, Prof. Dr. D. Li
Department of Chemistry and Multidisciplinary Research Center
Shantou University
Shantou 515063 (P.R. China)
Fax: (+86) 754-290-2767
E-mail: dli@stu.edu.cn

[**] This work was partly supported by the National Natural Science Foundation of China (Nos. 20571050 and 20271031), the China Postdoctoral Science Foundation, and the NSF of Guangdong Province (No. 05300875).

Supporting information for this article is available on the WWW under http://www.angewandte.org or from the author.

these vesicles have wrinkly surfaces as a result of shrinkage upon drying.

Hollow spheres of nanometer to submicrometer diameter have potential applications in controlled drug release, catalysis, chemical sensors, and cancer hyperthermia,[9] because of their many attractive characteristics, such as low density, larger surface areas, lower amount of material required, and low costs. Also, nanostructured alloys represent an interesting class of materials that exhibit properties distinct from the corresponding monometallic nanoparticles.[10,11] For example, PtRu[11a] and PtRuIr[11b] alloys exhibit enhanced electrocatalytic activity for fuel oxidation relative to pure Pt and are virtually immune to CO poisoning, which is often an intermediate of such reactions. As the properties are strongly dependent on the sizes, compositions, and morphologies of the particles, developing a simple and general approach for hollow alloy spheres with large surface areas and low density is essential for many practical purposes. However, compared with the various morphological controls of semiconductors, metals, and other inorganic materials, the production of bimetallic hollow spheres has met with only very limited success.[12,13] Hitherto, no hollow alloy sphere containing more than two kinds of metals has been reported. A major problem is how to control quick diffusion of different atoms to form homogeneous alloys while simultaneously forming hollow shells.

As Bu_4NBr and some metal compounds or the mixture of these metal compounds can form vesicles with hollow structures, the vesicle surface should consist of numerous aggregated Bu_4N^+ cations and metal anions such as $[AuX_4]^-$, $[PdX_4]^{2-}$, $[PtX_6]^{2-}$, and $[Ag_nX_m]^{n-m}$ (X = Cl or Br). When these vesicles are reduced by $NaBH_4$, the newly formed metal nucleation sites with high reactivity are expected to diffuse quickly to form homogeneous alloys on the vesicle template. After growth of these nucleation sites, hollow alloy shells would form. A series of experiments were performed to test this hypothesis. Herein, we select the quaternary alloy AuPdPtAg as an example to demonstrate the efficiency of this novel vesicle-directed alloying strategy.

The hollow alloy spheres were obtained by direct reduction (with $NaBH_4$) of the turbid solution containing $PdCl_2$, $K[AuCl_4]$, $AgNO_3$, $K_2[PtCl_6]$, and Bu_4NBr. The structure and morphology of the AuPdPtAg sample were investigated by TEM and SEM. As shown in Figure 3, the centers of the spheres are brighter than the edges, which indicates that their interiors are hollow. The hollow spheres are approximately 500 nm in diameter, which is comparable with the size of the vesicles before reduction. Owing to the very thin shells, some spheres were cracked or collapsed after sonication during purification. Both the selected area electron diffraction (SAED) pattern (Figure 3b) and XRD data (Figure 4a) were consistent with a single-phase face-centered cubic (fcc) structure. The broad peaks in the XRD patterns indicate the small sizes of nanocrystals. The average particle size, calculated from the Scherrer equation, is approximately 4.6 nm. A magnified view of the hollow spheres showed that the shell was composed of many crystallized particles with sizes of 4–7 nm, which agrees well with the XRD data. The high-resolution transmission electron microscopy (HRTEM) image (Figure 3d) of a small particle shows uniform, well-resolved interference fringe spacing (ca. 0.235 nm) and implies that the four kinds of metal atoms diffused quickly to form a homogeneous alloy with highly crystalline structure. The composition was studied by energy-dispersive X-ray

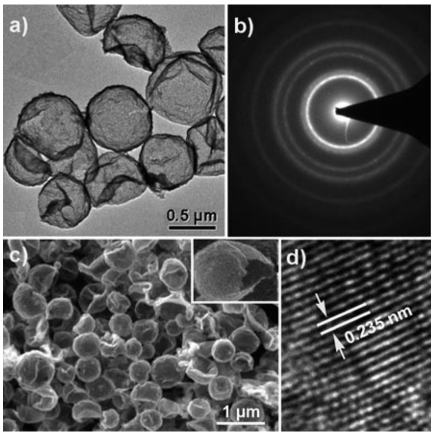

Figure 3. Characterization of hollow AuPdPtAg spheres. a) TEM image; b) SAED pattern; c) SEM image; Inset: enlarged view of a cracked sphere showing the thin shell; d) HRTEM image.

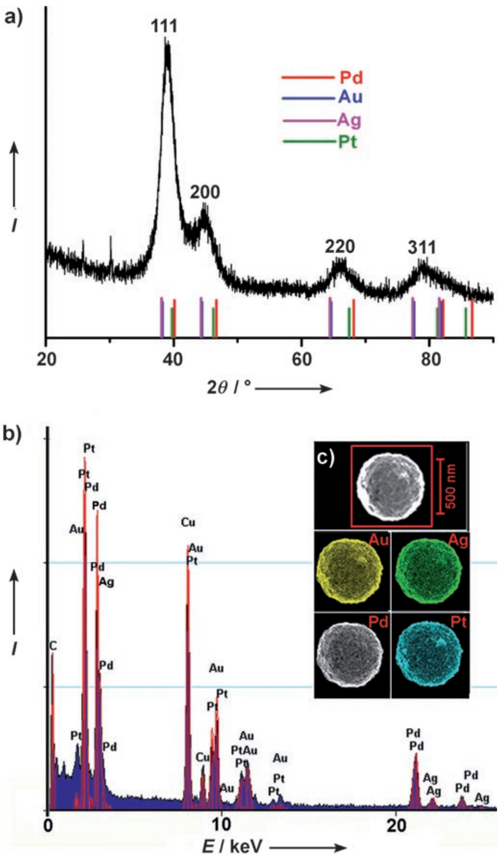

Figure 4. a) XRD pattern; b) EDX spectrum; c) Elemental mapping of hollow AuPdPtAg spheres.

(EDX) analysis. All of the Au, Pd, Pt, and Ag peaks could be seen clearly from the spectrum (Figure 4b). Elemental mapping data for a single sphere (Figure 4c) also indicated that the hollow sphere contained all of the four kinds of metals. The average stoichiometry was $Pd_{43}Au_{27}Pt_{19}Ag_{11}$ according to the EDX data. The X-ray photoelectron spectroscopy (XPS) binding energies (see the Supporting Information) were 335.7/341.95, 83.9/87.65, 71.75/75.1, and 368.0/373.95 eV for Pd $3d_{5/2,3/2}$, Au $4f_{7/2,5/2}$, Pt $4f_{7/2,5/2}$, and Ag $3d_{5/2,3/2}$, respectively, with some shifts relative to the data for the pure metals.[14] These shifts are often observed upon alloy formation[13a,14b] and proposed to be due to some interatomic charge donation between different elements, together with some intraatomic charge distribution.[15] As a result, the XRD, SAED, HRTEM, XPS, EDX data coupled with elemental mapping confirmed the formation of hollow spheres of AuPdPtAg alloy.

Some control experiments were implemented to verify this vesicle-directed co-alloying strategy further. It is known that micelles and vesicles formed in water can be destroyed by organic solvents such as alcohols. The result of an experiment in ethanol instead of water (other conditions keep constant) revealed that no hollow sphere formed (see the Supporting Information). Sonication of the reactants (in water) for 2 min before the addition of $NaBH_4$ resulted in some shapeless product, which suggested that the vesicles formed in this system could also be destroyed by sonication. When the experiments were carried out in water by replacing Bu_4NBr with Et_4NBr, only a very small amount ($<5\%$) of hollow spheres were produced, and none were produced with Me_4NBr, as evidenced by SEM images. This is probably due to the shorter alkyl chains and low hydrophobicity of Et_4NBr and Me_4NBr, which cannot assembly effectively into vesicles.

This vesicle-directed alloying strategy has been successfully extended to the synthesis of other bimetallic and multimetallic hollow spheres, such as PdAu, AuPt, AgPd, AuAg, PdAuPt, PdAuAg, PtPdRu, CoPdPt, and AuAgPdPt. Figure 5 shows the TEM and SEM images of some representative examples. Very interestingly, the sizes of the hollow spheres can be tuned by changing the types of metal in the alloys. We found that Ag decreases the size of the spheres, whereas Pt evidently increases the sphere sizes. For example, under the same synthetic conditions, the sizes of AuPdAg and AuPdPt are 90–150 nm and 200–550 nm, respectively. These differences are reasonable, as microstructures of vesicles are often composition-dependent and can be influenced by the geometries, concentrations, and charges of the counteranions or metal ions.[6,7] Although a higher ratio of one metal precursor always leads to a higher ratio of this metal in the final alloys, the metal ratios in hollow alloy spheres are not identical with those in the solution before reduction, probably because of the lattice mismatch of the different metals.

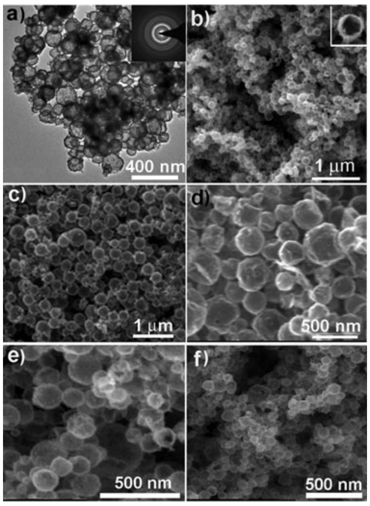

Figure 5. Representative hollow alloy spheres: a) TEM image of AuPdAg; Inset: SAED pattern. SEM images of: b) AuPdAg; Inset: enlarged view of a broken hollow sphere; c) CoPtPd; d) AuPdPt; e) PdAu; f) PdAg.

Although some transition-metal compounds such as $CoCl_2$, $RuCl_3$, and $K_2[PtCl_6]$ do not induce vesicle formation in this system, the metals Co, Ru, and Pt alloy efficiently with Au and Pd in systems containing vesicles induced, for example, by $PdCl_2$ and $K[AuCl_4]$ with reduction by $NaBH_4$. The reason is that, in the presence of excess Bu_4NBr, these metal compounds can form coordination anions ($[CoX_4]^{2-}$, $[RuX_6]^{3-}$, $[PtX_6]^{2-}$; X = Cl or Br) that can also be efficiently gathered onto the vesicle surface (induced, for example, by $PdCl_2$ and $K[AuCl_4]$) by electrostatic interactions with Bu_4N^+ ions on the surface. After reduction, these metal species alloy effectively with others. Hollow alloy spheres of CoPdPt, RuPtPd, AuPt, and others have been prepared in this way.

In conclusion, metal-compound-induced vesicles of Bu_4NBr were used as efficient directors for the rapid synthesis of hollow alloy spheres. This alloying strategy at the vesicle surface is general and has extended to the synthesis of a large variety of binary, ternary, and quaternary intermetallic materials with hollow structures. To our knowledge, this is the first time that different metals have been alloyed on a vesicle surface and that hollow alloy spheres containing more than two kinds of metals have been synthesized. This method could potentially be used for the rapid synthesis of other important alloy catalysts or semiconductors with hollow structures as well as changeable sizes and compositions.

Experimental Section

Typical synthetic procedure for hollow alloy spheres: AuPdPtAg: An aqueous solution of Bu_4NBr (30 mL, 0.01 M) was added to a mixture of $K[AuCl_4]$ (2.4 mL, 5×10^{-3} M in H_2O), $PdCl_2$ (1.6 mL, 0.01 M in acetonitrile), K_2PtCl_6 (1.6 mL, 5×10^{-3} M in H_2O), and $AgNO_3$ (0.8 mL, 5×10^{-3} M in H_2O). The solution was stirred for 3 min, and a freshly prepared $NaBH_4$ solution (2 mL, 0.1 M) was then added quickly. The mixture was stirred vigorous for 1 min, and the product was collected by centrifugation and washed with water. For the vesicle measurements, the solution was used directly for TEM and SEM analysis before addition of $NaBH_4$. When a drop of solution dries, a membrane always forms, which make the SEM analysis difficult. To avoid this problem, a drop of turbid solution was transferred onto a carbon-coated Cu grid, and excess solution was then absorbed and dried with filter paper before the SEM analysis. X-ray power diffraction (XRD) measurements of the samples were performed on a Rigaku D/max rA X-ray diffractometer with graphite-monochromated $Cu_{K\alpha}$ radiation ($\lambda = 1.54187$ Å) at a scanning rate of

0.06° s^{-1}. X-ray photoelectron spectroscopy (XPS) analysis was performed on VG Escalab 220i-XL spectrometer. TEM, HRTEM, EDX analysis, SAED, and elemental mapping were performed on TECNAI F30 high-resolution transmission electron microscope operated at 300 kV. SEM and field emission scanning electron microscopy (FE-SEM) were performed on JSM 6360 and PHILIPS XL30 scanning electron microscope, respectively. UV/Vis spectra were collected on a Philips PU-8620 UV/Vis spectrophotometer.

Received: April 25, 2006
Revised: July 3, 2006

Keywords: alloys · nanostructures · self-assembly · vesicles

---

[1] For reviews, see: a) D. M. Vriezema, M. C. Aragonès, J. A. A. W. Elmans, J. J. L. M. Cornelissen, A. E. Rowan, R. J. M. Nolte, *Chem. Rev.* **2005**, *105*, 1445, and references therein; b) M. Antonietti, S. Forster, *Adv. Mater.* **2003**, *15*, 1323; c) T. Dwars, E. Paetzold, G. Oehme, *Angew. Chem.* **2005**, *117*, 7338; *Angew. Chem. Int. Ed.* **2005**, *44*, 7174.

[2] a) D. E. Discher, A. Eisenberg, *Science* **2002**, *297*, 967; b) L. F. Zhang, A. Eisenberg, *Science* **1995**, *268*, 1728; c) S. Q. Zhou, C. Burger, B. Chu, M. Sawamura, N. Nagahama, M. Toganoh, U. E. Hackler, H. Isobe, E. Nakamura, *Science* **2001**, *291*, 1944.

[3] a) D. H. W. Hubert, M. Jung, A. L. German, *Adv. Mater.* **2000**, *12*, 1291; b) D. H. W. Hubert, M. Jung, P. M. Frederik, P. H. H. Bomans, J. Meuldijk, A. L. German, *Adv. Mater.* **2000**, *12*, 1286; c) B. M. Discher, Y.-Y. Won, D. S. Ege, J. C.-M. Lee, F. S. Bates, D. E. Discher, D. A. Hammer, *Science* **2001**, *294*, 1143.

[4] T. Ueno, M. Suzuki, T. Goto, T. Matsumoto, K. Nagayama, Y. Watanabe, *Angew. Chem.* **2004**, *116*, 2581; *Angew. Chem. Int. Ed.* **2004**, *43*, 2527.

[5] T. Rispens, J. B. F. N. Engberts, *Org. Lett.* **2001**, *3*, 941.

[6] a) C. A. Bunton, F. Nome, F. H. Quina, L. S. Romsted, *Acc. Chem. Res.* **1991**, *24*, 357; b) R. Zana, J. Schmidt, Y. Talmon, *Langmuir* **2005**, *21*, 11628.

[7] a) T. A. Waggoner, J. A. Last, P. G. Kotula, D. Y. Sasaki, *J. Am. Chem. Soc.* **2001**, *123*, 496; b) X. Luo, S. Wu, Y. Liang, *Chem. Commun.* **2002**, 492; c) T. Owen, R. Pynn, J. S. Martinez, A. Butler, *Langmuir* **2005**, *21*, 12109; d) J. Hao, J. Wang, W. Liu, R. Abdel-Rahem, H. Hoffmann, *J. Phys. Chem. B* **2004**, *108*, 1168.

[8] a) T. Liu, E. Diemann, H. Li, A. W. M. Dress, A. Müller, *Nature* **2003**, *426*, 59; b) T. Liu, *J. Am. Chem. Soc.* **2003**, *125*, 312.

[9] a) F. Caruso, *Chem. Eur. J.* **2000**, *6*, 413; b) E. Mathiowitz, J. S. Jacob, Y. S. Jon, G. P. Carino, D. E. Chickering, P. Chaturvedi, C. A. Santos, K. Vijayaraghavan, S. Montgomery, M. Bassett, C. Morrell, *Nature* **1997**, *386*, 410; c) Y. Hu, X. Q. Jiang, Y. Ding, Q. Chen, C. Z. Yang, *Adv. Mater.* **2004**, *16*, 933; d) C. Loo, A. Lin, L. Hirsch, M.-H. Lee, J. Barton, N. Halas, J. West, R. Drezek, *Technol. Cancer Res. Treat.* **2004**, *3*, 33.

[10] a) F. Maroun, F. Ozanam, O. M. Magnussen, R. J. Behm, *Science* **2001**, 293, 1811; b) S. Sun, C. B. Murray, D. Weller, L. Folks, A. Moser, *Science* **2000**, *287*, 1989.

[11] a) J. Huang, Z. Liu, C. He, L. M Gan, *J. Phys. Chem. B* **2005**, *109*, 16644; b) S. Liao, K.-A. Holmes, H. Tsaprailis, V. I. Birss, *J. Am. Chem. Soc.* **2006**, *128*, 3504.

[12] a) H.-P. Liang, Y.-G. Guo, H.-M. Zhang, J.-S. Hu, L.-J. Wan, C.-L. Bai, *Chem. Commun.* **2004**, 1496; b) H.-P. Liang, L.-J. Wan, C.-L. Bai, L. Jiang, *J. Phys. Chem. B* **2005**, *109*, 7795; c) Y. Sun, B. Wiley, Z.-Y. Li, Y. Xia, *J. Am. Chem. Soc.* **2004**, *126*, 9399.

[13] a) Y. Vasquez, A. K. Sra, R. E. Schaak, *J. Am. Chem. Soc.* **2005**, *127*, 12504; b) P. R. Selvakannan, M. Sastry, *Chem. Commun.* **2005**, 1684; c) G. S. Metraux, Y. C. Cao, R. Jin, C. A. Mirkin, *Nano Lett.* **2003**, *3*, 519; d) J. B. Liu, W. Dong, P. Zhan, S. Z. Wang, J. H. Zhang, Z. L. Wang, *Langmuir* **2005**, *21*, 1683.

[14] a) D. Briggs, M. P. Seah, *Practical Surface Analysis by Auger and X-ray Photoelectron Spectroscopy*, Wiley, Chichester, **1983**, p. 495; b) H. Gao, J. Y. S. Lin, Y. Li, B. Zhang, *J. Membr. Sci.* **2005**, *265*, 142, and references therein.

[15] a) A. Bzowski, T. Sham, *Phys. Rev. B* **1993**, *49*, 7836; b) C.-W. Yi, K. Luo, T. Wei, D. W. Goodman, *J. Phys. Chem. B* **2005**, *109*, 18535.